NASA Contractor Report 172555

NASA-CR-172555
19850014745

Investigation of Parabolic Computational Techniques for Internal High-Speed Viscous Flows

O.L. Anderson, G.D. Power

United Technologies Research Center
East Hartford, CT. 06108

Contract NAS1-17561

April 1985

National Aeronautics and
Space Administration

Langley Research Center
Hampton, Virginia 23665

Investigation of Parabolic Computational Techniques for Internal High-Speed Viscous Flows

TABLE OF CONTENTS

		Page
ACKNOWLEDGEMENT		ii
1.0	SUMMARY	1
2.0	INTRODUCTION	2
3.0	ANALYSIS	4
	3.1 Governing Equations and Solution Algorithm	4
	3.2 Characteristic Analysis	7
	3.3 Branching	9
4.0	RESULTS AND DISCUSSION	10
	4.1 Results of Flows Without Heat Addition.	10
	4.2 Results of Flow With Heat Addition	12
5.0	CONCLUDING REMARKS	14
6.0	LIST OF SYMBOLS.	15
7.0	REFERENCES	17
8.0	FIGURES	19

ACKNOWLEDGEMENT

The authors wish to acknowledge the contributions of Drs. M. Barnett and M. J. Werle of UTRC and Prof. F. T. Smith of University College, London. In addition, the authors note that the characteristic analysis and search for branching solutions discussed in this report were the result of independent research activities of UTRC.

1.0 SUMMARY

A feasibility study has been conducted to assess the applicability of an existing parabolic analysis (ADD-Axisymmetric Diffuser Duct), developed previously for subsonic viscous internal flows, to mixed supersonic/subsonic flows with heat addition simulating a SCRAMJET combustor. A study was conducted with the ADD code modified to include additional convection effects in the normal momentum equation when supersonic expansion and compression waves were present. A set of test problems with weak shock and expansion waves have been analyzed with this modified ADD method and stable and accurate solutions were demonstrated provided the streamwise step size was maintained at levels larger than the boundary layer displacement thickness. Calculations made with further reductions in step size encountered departure solutions consistent with strong interaction theory. Calculations were also performed for a flow field with a flame front in which a specific heat release was imposed to simulate a SCRAMJET combustor. In this case the flame front generated relatively thick shear layers which aggravated the departure solution appearance. Qualitatively correct results were obtained for these cases using the marching technique with the convective terms in the normal momentum equation suppressed. It is concluded from the present study that for the class of problems where strong viscous/inviscid interactions are present a global iteration procedure is required.

2.0 INTRODUCTION

An analysis for the prediction of supersonic internal flow fields with heat addition is required to support the development of SCRAMJET engine configurations by generating design information and by evaluating test data. Certain requirements should be met in order for this analysis to be applicable to a wide range of SCRAMJET configurations. First, the analysis should be able to treat mixed supersonic/subsonic flow fields because the boundary layers are subsonic and because realistic rates of heat addition may reduce the flow velocity to subsonic conditions behind the flame front. The analysis should be able to treat transverse pressure gradients produced by expansion waves, compression waves, and shock waves. Heat addition may also produce transverse pressure gradients. In addition, although not addressed in this study, the analysis should be able to treat hydrocarbon combustion chemistry with multi-species product gases and turbulent mixing controlled reactions. Finally the analysis should be three dimensional since almost all SCRAMJET configurations are three dimensional. These requirements place a great burden on the type of analysis that should be developed, on the solution algorithms required, and on the computer hardware. In the present feasibility study, only the first and second requirements were considered.

Forward marching procedures are attractive for supersonic internal flows since they require less computer time and storage than solution techniques required for the full Navier-Stokes equations. The successful implementation of these schemes, often referred to as parabolic methods, involves a fundamental problem in fluid mechanics, namely numerical instabilities which arise in parabolic codes and which are associated with upstream propagation in viscous interaction regions of the flow field. Existing analyses, such as those developed in Refs. 1 and 2, are unable to adequately treat this problem which may be described in the following manner. In supersonic flow, the inviscid Euler equations can be solved by forward marching numerical methods because there is no upstream propagation of information. In subsonic flow upstream propagation always exists and hence forward marching solutions are inherently unstable. However, in viscous interacting supersonic flow, portions of the boundary layer admit some upstream propagation; hence, forward marching solutions of the parabolized Navier-Stokes equations are unstable. Successful methods have been developed for suppressing these instabilities in two dimensional flows by modifying the streamwise pressure gradient in subsonic regions in an approximate manner (see Refs. 3-8). Similarly, in subsonic two dimensional flow fields parabolic solution techniques can be employed for the composite inviscid/viscous equations by treating the streamwise pressure gradient in some appropriate manner as was done in Ref. 9. While such techniques have a numerical attractiveness, they force a compromise of the physics of the problem by eliminating the streamwise pressure gradient over a finite region of the flow field - a region that would be sizable in a SCRAMJET combustor where heat addition may produce large regions of embedded subsonic flow.

Another method which is stable for forward marching solutions of an approximate form of the Navier-Stokes equations is the ADD (Axisymmetric Diffuser Duct) approach (Refs. 10 and 11) which has been demonstrated for a wide range of problems in subsonic viscous duct flow (Ref. 12) and in supersonic jet flows with subsonic coflowing outer streams (Ref. 13). This method provides the starting point for the present study. In the ADD approach a parabolic set of equations are obtained by writing the governing equations in an intrinsic coordinate system that approximates the actual streamlines. The use of this coordinate system permits the deletion of the convection terms in the normal momentum equation since the coordinate curvature approximates the streamline curvature. The resulting set of equations have been shown to be formally parabolic and devoid of branching solutions (Ref. 11) and, thereby, result in a stable forward marching procedure with the pressure allowed to vary across the viscous flow subject to a specificed streamline curvature. The essential issue is that branching is avoided by control of the normal pressure gradient at the outer edge of the viscous interacting layer. The applicability of this concept to SCRAMJET combustors is verified here for model flow problems with and without heat addition. Additionally, since the complex flow field in a SCRAMJET combustor makes it difficult to obtain an a priori good approximation to the streamline curvature, this issue is addressed in a limited way. In this study an investigation was conducted of a means of improving the streamline curvature approximation while still controlling the imbedded instability of the interacting flow using the method of Ref. 11 by controlling the convection terms in the transverse momentum equations.

3.0 ANALYSIS

3.1 Governing Equations and Solution Algorithm

Basic Equations

The derivation of the governing equations which comprise the basic ADD approach are given by Anderson (Ref. 11). These equations are written in a general orthogonal coordinate system which is constructed from incompressible plane potential flow in which the velocity potential is the streamwise coordinate and the stream function is the normal coordinate. The Navier-Stokes equations are then parabolized by assuming the velocity component normal to the streamwise coordinate (incompressible potential flow streamline) is small compared to the streamwise velocity component. Thus we have a coordinate system in which one set of coordinate lines are the incompressible streamlines which serve as a first order approximation of the streamlines in subsonic flow. Figure 1 shows a schematic diagram of the coordinate system and definition of curvature for a typical duct.

The basic parabolized Navier-Stokes equations used in the ADD code (Ref. 11) are given as follows:

continuity

$$\frac{\partial \psi}{\partial n} = hr\rho U_s \tag{1a}$$

$$\frac{\partial \psi}{\partial s} = -hr\rho U_n \tag{1b}$$

s-momentum

$$\frac{\rho U_s}{h}\frac{\partial U_s}{\partial s} + \frac{\rho U_n}{h}\frac{\partial U_s}{\partial n} - K_s\,\rho U_n U_s + \frac{1}{h}\frac{\partial P}{\partial s} - \frac{1}{rh^2}\frac{\partial}{\partial n}\left(hr\tau_{ns}\right) + K_s\tau_{ns} = 0 \tag{2}$$

n-momentum

$$\left\{\frac{\rho U_s}{h}\frac{\partial U_n}{\partial s} + \frac{\rho U_n}{h}\frac{\partial U_n}{\partial n}\right\} + K_s \rho U_s U_s + \frac{1}{h}\frac{\partial P}{\partial n} = 0 \tag{3}$$

energy

$$\frac{\rho U_s}{h}\frac{\partial I}{\partial s} + \frac{\rho U_n}{h}\frac{\partial I}{\partial n} + \frac{1}{rh^2T}\frac{\partial}{\partial n}(rhq) - \frac{1}{T}\tau_{ns}\frac{\partial}{\partial n}\left(\frac{U_s}{h}\right) - \frac{\dot{q}}{T} = 0 \tag{4}$$

shear stress

$$\tau_{ns} = \mu_T \frac{\partial}{\partial n}\left(\frac{U_s}{h}\right) \tag{5}$$

heat flux

$$q = \frac{-\lambda_T}{h}\frac{\partial T}{\partial n} \tag{6}$$

entropy

$$I = \frac{\gamma}{\gamma-1}\ln\left(\frac{T}{T_r}\right) - \ln\left(\frac{P}{P_r}\right) \tag{7}$$

state

$$P = \rho RT. \tag{8}$$

Thus we have a set of eight equations for eight dependent variables (U_s, ψ, τ_{ns}, q, P, T, ρ, I), where the normal velocity component U_n is eliminated using Eq. (1b). In order to model the effect of heat addition, a source term $\dot{q}/T$ has been added to Eq. (4). For the purpose of the current study, this heat addition was specified a priori throughout the duct. In subsonic flow, K_s, the coordinate curvature, is a good approximation to the actual streamline curvature and the bracketed terms in Eq. (3) may be neglected. However, supersonic flow can only be turned by expansion/compression waves or

inclined shock waves; therefore, in supersonic flow, the streamline curvature differs significantly from the coordinate curvature (K_s) as computed from an incompressible theory and a correction is needed. Vatsa et al. (Ref. 13) found that for some supersonic flows a simple linear theory could be employed to approximate K_s. However, in general supersonic cases this approximation will not be sufficient and the bracketed terms must be included.

Boundary Conditions and Initial Conditions

The initial conditions for this problem require specification of all dependent variables U_s, U_n, ψ, τ_{ns}, q, P, T, ρ, I on the inlet plane. The normal velocity U_n is added to this list since its derivative with respect to s now appears in the equations in the bracketed term of Eq. (3). In the free stream, it is assumed that τ_{ns}, q, and U_n are zero. The remaining variables are uniquely defined by specifying $U_s(n)$, P(n), and T(n) and using isentropic flow relations and continuity (Eq. 1a). In the boundary layer, Cole's wall-wake law (Ref. 14) is used to determine initial conditions consistent with the turbulence model (Ref. 11).

The boundary conditions for these equations are given as follows:

inside diameter wall:

$$\left.\begin{aligned} U_s &= 0 \\ q &= 0 \\ \psi &= 0 \end{aligned}\right\} \qquad (9)$$

outside diameter wall:

$$\left.\begin{aligned} U_s &= 0 \\ q &= 0 \\ \psi &= \text{constant} \end{aligned}\right\} \qquad (10)$$

Solution Algorithm

When the turbulent viscosity (μ_T) is properly modeled and the inlet mean flow is specified, Eqs. (1)-(8) can be solved by a forward marching integration scheme. Equations (1)-(8) are first linearized by expanding all dependent

variables in a Taylor series expansion in the marching direction (s), and dropping terms of O (Δs^2). Finite difference equations are then obtained using the two point centered difference scheme of Keller (Ref. 15). Figure 2 shows the finite difference modules corresponding to the finite difference equations solved in the ADD code. Figure 2a is a schematic of the finite difference module related to all of the ADD code equations except the normal momentum equation, Eq. (3). Figure 2b shows the finite difference module for the normal momentum equation used in the subsonic version of the ADD code. In the present version, Eq. (3), however, uses a modified box scheme which employs a centered difference in the normal direction and a three point backward difference in the streamwise direction (see Fig. 2c). The resulting matrix equations are block tridiagonal and are solved by block factorization using the method of Varah (Ref. 16).

3.2 Characteristic Analysis

Following the method of Ref. 17, the characteristic determinant of Eqs. (1)-(8) can be shown to be:

$$D = -\lambda_T \mu_T^2 \left(\frac{1}{h}\frac{\partial \alpha}{\partial s}\right)^4 \left[\frac{\{\Omega\}\Omega}{T} - R\,\frac{1}{h}\frac{\partial \alpha}{\partial n}\right]^2 \tag{11}$$

where α (n,s) is a characteristic line, R the gas constant, T the temperature, and

$$\Omega = \frac{U_s}{h}\frac{\partial \alpha}{\partial s} + \frac{U_n}{h}\frac{\partial \alpha}{\partial n} \tag{12}$$

If the bracketed term of Eq. (3) is dropped, the characteristic determinant for the original ADD code is recovered by recognizing that the bracketed term in Eq. (11) does not appear and thus,

$$D = -R\lambda_T \mu_T^2 \left(\frac{1}{h}\frac{\partial \alpha}{\partial s}\right)^6 \tag{13}$$

This result, (Eq. 13), implies that the ADD code equations are formally parabolic, since all six roots of Eq. (13) are equal and real. Additionally, as pointed out in Ref. 11, these equations are devoid of viscous interaction branching solutions and a forward marching numerical procedure can be used.

Returning now to the characteristic roots of the full equations, Eq. (11), the relationship between temperature (T) and speed of sound (a) is introduced, and the determinant in Eq. (11) is set to zero. Then we have:

$$\frac{1}{h}\frac{\partial\alpha}{\partial s} = -\left(\frac{U_n}{U_s} \pm \sqrt{\frac{a^2}{\gamma U_s^2}}\right)\frac{1}{h}\frac{\partial\alpha}{\partial n} \tag{14a}$$

$$\left(\frac{1}{h}\frac{\partial\alpha}{\partial s}\right)^4 = 0 \tag{14b}$$

Thus for a full set of equations (Eqs. 1 to 8), four roots are real and equal, Eq. (14b), and two roots are real and unequal, Eq. (14a).

Additionally note that for the subcharacteristics, which are the characteristics of the inviscid flow, the determinant can be shown to be:

$$D = C_p\rho^2\Omega^2\left\{\left[\left(\frac{U_s}{a}\right)^2 - 1\right]\left(\frac{1}{h}\frac{\partial\alpha}{\partial s}\right)^2 + 2\,\frac{U_s}{a}\frac{U_n}{a}\left(\frac{1}{h}\frac{\partial\alpha}{\partial s}\right)\left(\frac{1}{h}\frac{\partial\alpha}{\partial n}\right) + \left[\left(\frac{Un}{a}\right)^2 - 1\right]\left(\frac{1}{h}\frac{\partial\alpha}{\partial n}\right)^2\right\} \tag{15}$$

In this case, two roots are real and unequal in supersonic flow and complex in subsonic flow and easily identified with the Mach lines. The remaining two roots (Ω=0) are the streamlines.

This characteristic analysis leads one to expect certain properties in the forw rd marching numerical solution of the mixed supersonic/subsonic flow problem based on the dominant characteristics in each flow regime. For internal flows without heat addition, the flow field consists of a supersonic, essentially inviscid core flow, and a viscous, partly subsonic, boundary layer flow (as shown schematically on Fig. 3). Therefore the core flow (R_3) is dominated by the real subcharacteristics of Eq. (15), and one would expect forward marching solutions to be possible. The wall boundary layer, however, is viscous and therefore governed by Eq. (11) and the characteristic roots of equations (14a) and (14b). Formally this implies a parabolic/hyperbolic mixed flow which one might expect to be well posed as an initial value problem. Note that the fact that the subcharacteristic analysis of Eq. (15) might imply ill possessedness in the subsonic region is not directly applicable because such is true only near the wall where

the viscous terms are active and thus Eqs. (14) hold. Therefore the characteristic analysis does not provide a clear picture of how to establish a well posed problem and solution algorithm for such viscous interacting flows. However, interaction theory does provide some guidelines that will be discussed below.

3.3 Branching

The concepts of branching solutions which occur in viscous interaction problems has been discussed by numerous previous authors and is well summarized in the recent work of Barnett (Ref. 18) for external flows and by Smith (Ref. 19) for internal flows. The essential issue is that all viscous interaction equations (subsonic or supersonic) are illposed as initial value problems because they contain imbedded eigenvalue solutions (branching solutions) with scale lengths shorter than a boundary layer thickness. This family of solutions represents the strong interaction situations where some physical event causes the viscous region to significantly modify the overlaying inviscid flow such as separation of the boundary layer. In situations where this is not expected to occur, such branching solutions may be suppressed using numerical expedients to purge short length scale solutions. Thus for example, Barnett (Ref. 18) found that the eigenvalue solution could be formally eliminated for supersonic flows by suppressing the longitudinal pressure gradient term of Eq. (2) at the wall. Anderson (Ref. 11) used the conclusions of Smith (Ref. 19) to suppress and avoid branching in subsonic channel flow by controlling the normal pressure gradient in the viscous/inviscid overlap region at the boundary layer edge.

In SCRAMJET combustors, a major dilemma again occurs because a mixed situation appears in a more pronounced form. Boundary layers develop along the walls under supersonic portions of the core flow. In addition the flame front produces large temperature gradients and because heat addition decelerates the flow, large shear layers are also produced through the flame front. With sufficient heat addition, the flow becomes subsonic. Thus the region of viscous/inviscid interaction is greatly expanded (see Fig. 3). Since this latter effect is dominant in SCRAMJET combustors, attention was focused on the use of subsonic strategies to address the branching issue. Thus attention has been focused only on the normal pressure gradient effects for the present limited scope study. To this end in fully subsonic flows the bracketed terms of Eq. (3) are neglected and the normal pressure gradient is determined by the curvature term K_s. In supersonic regions of the flow, the bracketed terms are included to allow modification of the streamline curvature over those of the incompressible streamline curvature. The expectation would be that the resulting set of equations would still contain branching solutions since they contain all the interacting effects in the overlap region at the viscous layer edge.

4.0 RESULTS AND DISCUSSION

4.1 Results of Flows Without Heat Addition

Expansion Wave Case

The first model problem was selected to demonstrate that a forward marching numerical method exists for mixed subsonic/supersonic flow when the bracketed terms in Eq. (3) are treated properly, and that the modified equations can model the behavior of flow turning by expansion waves. The model problem was a two dimensional duct with a five degree expansion turn. This turn results in a centered Prandtl-Meyer expansion from the corner which reflects back and forth between the two walls as shown in Figs. 4 and 5. The inlet Mach number was 2.0, expanded from plenum conditions set at a standard atmosphere and with a prescribed normal velocity, $U_n = 0$. The initial turbulent boundary layer displacement thickness was 1.0 percent of the duct height, and the flow Reynolds number based on duct height was 1.2×10^6. The computational mesh consisted of a 50 x 50 grid in which the streamwise step size was such as to approximately satisfy the CFL (Courant-Friedrich-Levy) condition everywhere except in a thin region in the boundary layer. Two calculated results are shown for this configuration in Figs. 4 and 5.

Figure 4 shows the calculated wall pressure distribution using the original ADD code for the upper and lower walls, without the addition of the bracketed terms in Eq. (3), compared with the wall pressure distribution calculated using the one dimensional isentropic flow relations. This figure shows, as expected, that the incompressible coordinate curvature, K_s, (see Fig. 1) completely fails to model flow turning in supersonic flow. Downstream from the corner where K_s is small, the equations appear to model one dimensional flow with boundary layer blockage.

Figure 5 shows the results of a second calculation in which the convection terms (bracketed terms of Eq. (3)) are included in the supersonic regions of the flow and neglected in the subsonic regions of the flow. In this figure, the calculated wall pressure distribution for the upper and lower walls is compared to the wall pressure distribution calculated by the Method of Characteristics (MOC). In this case the supersonic flow field is properly modeled since the Prandtl-Meyer expansion is captured. The initial drop in pressure at the corner is very sharp and does not appear to cause numerical difficulties. The effect of blockage was calculated by using the method of characteristics on a new duct shape modified by the calculated displacement thickness. Figure 5 shows that the calculated wall pressure distribution agrees well with method of characteristics when blockage is included.

During the course of the investigation, it was found that, for large streamwise step sizes, the resulting pressure distribution exhibited oscillations about a mean pressure distribution. This behavior is typical of the Keller Box scheme for which the difference module is shown on Figs. 2a and 2b. As stated previously, the differencing of Eq. (3) was modified to reduce this oscillation using the difference module shown on Fig. 2c. Figure 6 shows a comparison between results calculated using the two schemes. All solutions given in this report were calculated using Eq. (3) in the modified difference form.

Figure 7 shows the effect of streamwise step size on the calculated pressure distribution on the outer wall. The streamwise step size ΔX is referenced to two nominal length scales. The first, ΔX_{CFL}, is that step size satisfying the CFL condition using the inlet centerline Mach number and ΔY grid spacing. The second, δ_o^*, is the inlet displacement thickness used as representative thickness of the wall boundary layer. The results shown in Fig. 7 indicate that the reduction of the streamwise step size sharpens the centered expansion wave, suggesting that some of the spreading of the wave relative to that calculated by the method of characteristics is due to truncation error.

Shock Wave Case

A second model problem was selected to demonstrate that the modified equations can capture the behavior of flow turning by shock waves. The model problem was a two dimensional duct with a five degree compression turn and a five degree expansion turn. The compression turn results in a shock wave which reflects off of the opposite wall as shown in Fig. 8. The inlet Mach number was 4.0 with initial conditions: P_T = 32143.5 psf, T_T = 2184°R, and U_n = 0. The initial turbulent boundary layer displacement thickness was 1.0 percent of the duct height, and the flow Reynolds number based on duct height was 1.4×10^6. As in the previous case, the computational mesh was constructed such that the CFL condition was approximately satisfied everywhere except for a thin region in the boundary layer.

Figure 8 shows the configuration and computed results for this model problem. In this figure, the calculated wall pressure distribution for the upper and lower walls is compared to the pressure distribution calculated by the method of characteristics. The shock wave and the Prandtl-Meyer expansion on the upper wall, as well as the reflected shock wave on the lower wall, are captured reasonably well. As in the previous case, the abrupt pressure changes do not seem to cause numerical instabilities for the streamwise step sizes chosen in this calculation. Figure 9 shows the effect of streamwise step size on the pressure distribution along the upper wall for this case. The steepening of the pressure changes near the compression and expansion turns, as in the previous case, indicate that the effect of truncation error is reduced for smaller step

sizes. Figure 10 shows the calculated streamlines for this configuration compared to the incompressible streamlines used as a streamwise coordinate. This figure shows that the additional terms included in the supersonic region allow the equations to model the actual flow even though the streamline curvature is significantly different from the incompressible streamline curvature.

Departure Solutions

Although the preliminary step size studies, presented in the previous sections, indicate that reducing the step size reduces the truncation error, it has not been demonstrated that with very small step sizes numerical instabilities called departure solutions actually occur. Towards this end a model problem was selected in which all extraneous phenomena such as shock waves or expansion waves were removed. The configuration was a two dimensional straight duct with an inlet Mach number of 2.0, expanded from plenum conditions set at a standard atmosphere and an inlet normal velocity, $U_n = 0$. The initial turbulent boundary layer displacement thickness was 1.0 percent of the duct height, and the flow Reynolds number based on the duct height was 1.2×10^6. Figure 11 shows the wall pressure distribution for this case at various values of streamwise step size. Note again, that the streamwise step size, ΔX, is referenced to the nominal length scales ΔX_{CFL} and δ_o^* defined earlier. At the two larger step sizes $\Delta X/\Delta X_{CFL} = 0.22$ and 0.11, the solution appears to be well behaved as a slight increase in pressure is observed downstream from the inlet due to boundary layer blockage. However, further reduction in the streamwise step size with a fixed y-grid produces results which differ significantly from the expected pressure rise.

One possible cause for these instabilities is suggested by the discussion on branching presented in Sec. 3.3. Barnett (Ref. 18) observed similar behavior and was able to show through detailed step size analysis that these branching solutions were precisely the exponentially growing eigenvalue solutions predicted by triple deck analysis for the viscous interaction equations embedded in the current composite equations. Thus it appears that the current equation set with the bracketed term of Eq. (3) included still contains the fundamental mechanisms for strong interaction effects. Branching solutions can thus be filtered by dropping the bracketed terms in Eq. (3) altogether or by keeping the streamwise step size large when it is retained. For flows in which strong interaction effects are believed to be important, a global iteration scheme would be required (see for example Ref. 18 and 21) to properly represent these viscous interaction effects.

4.2 Results of Flow With Heat Addition

A SCRAMJET model problem was selected to demonstrate that the numerical method was stable for heat addition in a mixed subsonic/supersonic flow and that the equations properly model the effect of the heat addition. The model was a

two dimensional straight duct with a majority of the mass flow (90%) in the free-stream (cold) portion of the duct at the initial plane and the remaining flow in the pilot (hot) portion of the duct. The combustion process was modeled by specifying the heat input per second ($\dot{q}$) as a function of axial distance and radius, thus defining a flame front. Figure 12 shows the configuration for this model problem. The UTRC Mixing and Combustion code (Ref. 20), currently being used in connection with another NASA contract to analyze SCRAMJET configurations, was used to determine realistic initial conditions, heat input, and flame front location. The inlet Mach number was 3.1 and 1.1 and the inlet stagnation temperature was 2200°R and 5000°R for the cold and hot portions of the duct, respectively. A constant static pressure of 1227.5 psf and normal velocity, U_n = 0, were also specified. Figure 13 shows the specified heat input which models the combustion process. Figure 13a shows how the heat input per second was spread over a small region about the flame midpoint and Fig. 13b shows the value of the maximum heat input at the flame midpoint as it varies with axial distance.

Figure 12 shows that there is a rise in static pressure when heat is added, as expected. Figure 14 and 15 are detailed plots of the static temperature and Mach number profiles at the inlet and exit planes, respectively. The extent of the cold portion of the duct has decreased considerably due to the heat addition. Note also that the flow is sheared over a majority of the duct. As this shear layer increases, it was found that the numerical method becomes unstable when the bracketed terms in Eq. (3) are included. This result is consistent with the characteristic analysis presented in Section 3.2 in that the existence of the flame front greatly enlarges the region (R_2) where the weakly elliptic characteristics dominate (see Fig. 3). The results shown here were calculated with these terms neglected. Since the streamline curvatures are nearly identical for incompressible and supersonic flow in this case, neglecting these terms should not effect the results. Additional work is needed to determine how to properly handle these terms for flows with large shear regions. Figures 16 and 17 show the static temperature and Mach number profiles, respectively, through the duct. The flame front can be clearly seen by the large gradients in its vicinity. As an additional check of the heat addition model, the total enthalpy change across the flame front was compared to the results of the UTRC Mixing and Combustion code. The ADD code gives:

$$\frac{\Delta H}{H_{in}} = 0.28$$

and the UTRC mixing and combustion code gives:

$$\frac{\Delta H}{H_{in}} = 0.29$$

5.0 CONCLUDING REMARKS

The subsonic parabolized Navier-Stokes technique used in Ref. 11 has been extended to treat mixed supersonic/subsonic flow fields in which the core flow is supersonic and the inner region of the boundary layer is subsonic. This extension to supersonic flow was made by including the convection terms in the normal momentum equation when the flow is supersonic and neglecting these terms when the flow is subsonic. Stable and accurate solutions have been demonstrated for weak shocks and expansion waves provided the streamwise step size is carefully selected. Calculations have also been obtained for a simulated SCRAMJET engine with a priori heat input which generates a large subsonic flow region downstream from the flame front. These latter calculations were found to be possible only when using the subsonic parabolized Navier-Stokes technique used in Ref. 11.

Departure solutions have been demonstrated for the mixed supersonic/subsonic flow field problem when the streamwise step size is of the order of the inlet displacement thickness or less. A characteristic analysis shows that the parabolized Navier-Stokes equations used in this analysis are always of the mixed hyperbolic/parabolic type whereas interaction theory indicates an illposed problem due to the inclusion of the convection terms in the normal momentum equation. Thus the possibility of instability (departure solutions) always exists and special strategies are required for suppression of such weak interaction solutions.

For SCRAMJET combustors, the flame front produces shear layers which greatly enlarge the region of viscous interaction and may with sufficient heating produce a subsonic region behind the flame front. To completely capture such strong interaction effects, it is believed that a global iteration procedure could be developed.

6.0 LIST OF SYMBOLS

a	Speed of sound
C_p	Specific heat
H	Enthalpy
H_{in}	Inlet enthalpy
h	Metric scale coefficient
I	Entropy
JL	Number of steps in streamwise direction
KL	Number of steps in normal direction
K_s	Curvature of coordinate streamline
n	Normal coordinate
P	Static pressure
P_r	Reference static pressure
P_T	Total pressure
q	Heat flux - dependent
$\dot{q}$	Heat flux added by combustion
r	Radial coordinate
s	Streamwise coordinate
T	Static temperature
T_r	Reference temperature
T_T	Total temperature
U_n	Normal mean velocity
U_s	Streamwise mean velocity
X	Streamwise direction

Y	Distance from lower wall
Y_f	Location of flame front
Y_T	Height of the duct
α	Characteristic direction
γ	Ratio of specific heats
ΔX	Streamwise step size
ΔX_{CFL}	Step size satisfying CFL condition
δ_o^*	Displacement thickness at inlet
λ_T	Effective turbulent thermal conductivity
Ω	See Equation 12
μ_T	Effective turbulent viscosity
ρ	Density
τ_{ns}	Shear stress
ψ	Stream function

7.0 REFERENCES

1. Dyer, D. F., G. Maples and D. B. Spalding: Combustion of Hydrogen Injected into a Supersonic Airstream, NASA CR-2655, 1976.

2. Zelazny, S. W., A. J. Baker and W. L. Rushmore: Modeling of Three Dimensional Mixing and Reacting Ducted Flows, NASA CR-~~2621~~ 2661, 1976.

3. Lin, T. C. and S. G. Rubin: A Numerical Model for Supersonic Viscous Flow Over a Slender Reentry Vehicle. AIAA Paper No. 79-0205, 17th Aero. Sciences Meeting, January 1979.

4. Lin, T. C. and S. G. Rubin: Viscous Flow Over a Cone at Moderate Incidence I, Int. J. of Computers and Fluids, Vol. 1, p. 37-57, 1973.

5. Vigneron, Y. C., J. V. Rakich, and J. C. Tannehill: Calculation of Supersonic Viscous Flow Over Delta Wings with Sharp Leading Edges. AIAA Paper No. 78-1137, 1978.

6. Rakich, J. V., R. T. Davis and M. Barnett: Simulation of Large Turbulent Structures with the Parabolic Navier-Stokes Equations. NASA TM 84262, June 1982.

7. Schiff, L. B. and J. L. Steger: Numerical Simulation of Steady Supersonic Viscous Flow. AIAA Paper No. 79-0130, 1979.

8. Barnett, M.: The Solution of the Parabolized Navier-Stokes Equations by a Fully Implicit Method. AIAA Paper No. 82-0415, 1982.

9. Rae, W. J.: Some Numerical Results on Viscous Low Density Nozzle FLows in the Slender Channel Approximation. AIAA J., Vol. 9, p. 811, 1971.

10. Anderson, O. L., G. B. Hankins and D. E. Edwards: Extension to an Analysis of Turbulent Swirling Compressible Flow for Application to Axisymmetric Small Gas Turbine Ducts. NASA CR-165597, February 1982.

11. Anderson, O. L.: Calculation of Internal Viscous Flows in Axisymmetric Ducts at Moderate to High Reynolds Number. Int. J. of Computers and Fluids, Vol. 8, No. 4, p. 391-411, December 1980.

12. Barber, T. J., P. Raghuraman and O. L. Anderson: Evaluation of an Analysis for Axisymmetric Internal Flows in Turbomachinery Ducts. Flow in Primary Non-Rotating Passages in Turbomachines. ASME Winter Annual Meeting, December 1979.

13. Vatsa, V. N., M. J. Werle, O. L. Anderson and G. B. Hankins, Jr.: Solutions for Three-Dimensional Over- or Underexpended Exhaust Plumes. AIAA Journal, Vol. 20, September 1982.

14. Coles, D.: The Law of the Wake in the Turbulent Boundary Layer. Journal of Fluid Mechanics, Vol. 1, 1956.

15. Keller, H. B.: A New Difference Scheme for Parabolic Problems, Numerical Solution of Partial Differential Equations II, SYNSPADE, 1970.

16. Varah, J. M.: On Solution of Block-Tridiagonal Systems Arising from Certain Finite Difference Equations. Math. Comp., Vol. 26, p. 120, 1972.

17. Courant, R. and D. Hilbert: Methods of Mathematical Physics, Vol. II - Partial Differential Equations, Interscience Publishers, 1972.

18. Barnett, M.: The Calculation of Supersonic Flows with Strong Viscous-Inviscid Interaction Using the Parabolized Navier-Stokes Equations, PHD Dissertation University of Cincinnati, 1984.

19. Smith, F. T.: Upstream Interactions in Channel Flows, J. Fluid Mechanics, Vol. 79 Part 4, 1977, pp. 631-655.

20. McVey, J. B., J. B. Kennedy, and F. L. Haviland: Hydrocarbon-Fueled SCRAMJET, Vol. IX Combustor Design Procedures, AFAPL-TR-68-146, August 1971.

21. Presz, W. Jr.: A Numerical Method for Channel Flow with Separation, UTRC Report No. 84-49, April 1985.

8.0 FIGURES

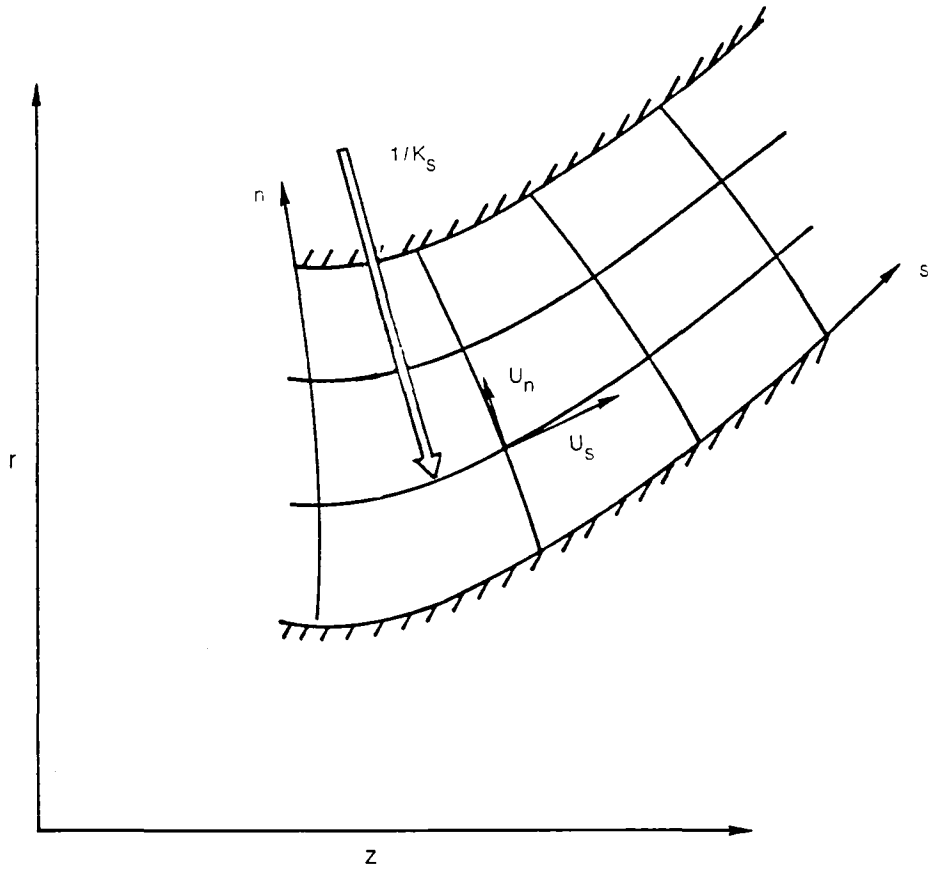

Fig. 1 Coordinate System and Curvature

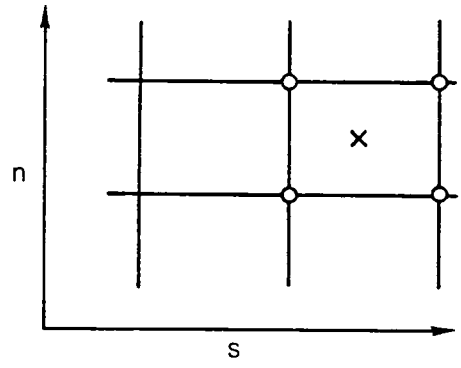

a. KELLER BOX SCHEME

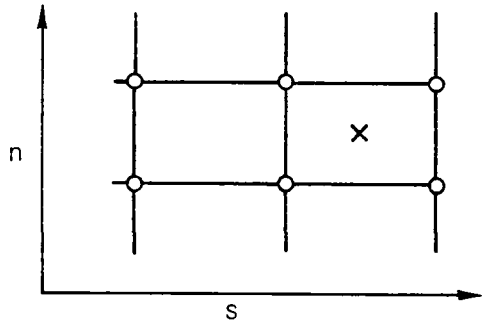

b. BOX SCHEME FOR NORMAL MOMENTUM EQUATION

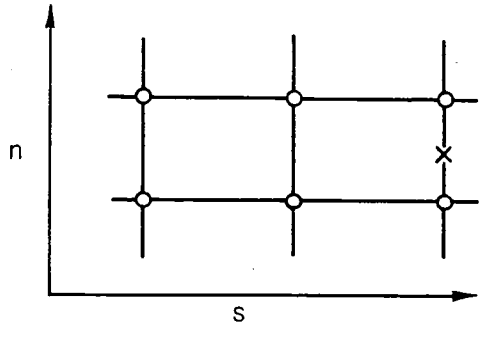

c. MODIFIED BOX SCHEME FOR NORMAL MOMENTUM EQUATION

Fig. 2 Finite Difference Modules

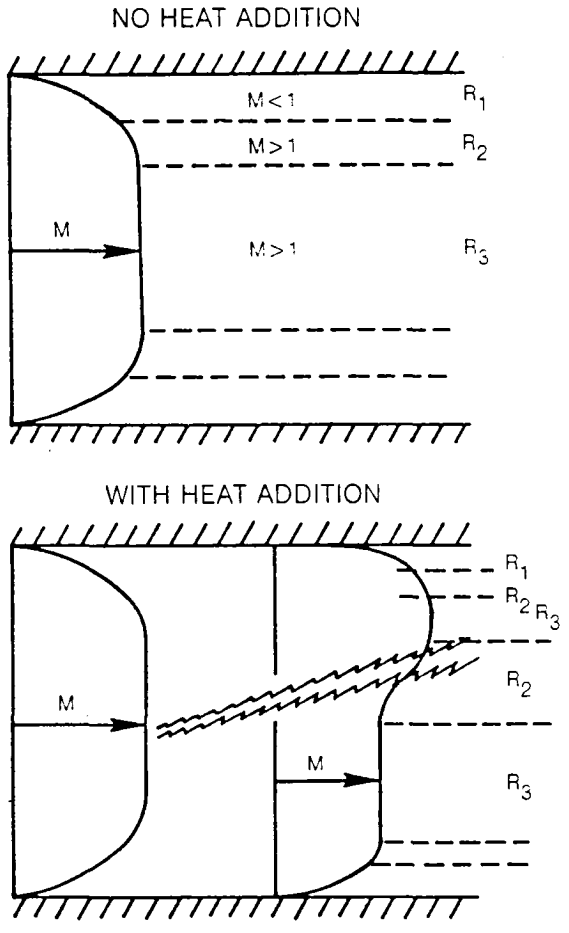

R_1	R_2	R_3
$M<1$	$M>1$	$M>1$
$\tau>0$	$\tau>0$	$\tau=0$
$\{\Omega\}=0$	$\{\Omega\}\neq 0$	$\{\Omega\}\neq 0$
PARABOLIC	WEAKLY HYPERBOLIC	HYPERBOLIC

Fig. 3 Flow Regions and Dominant Characteristics

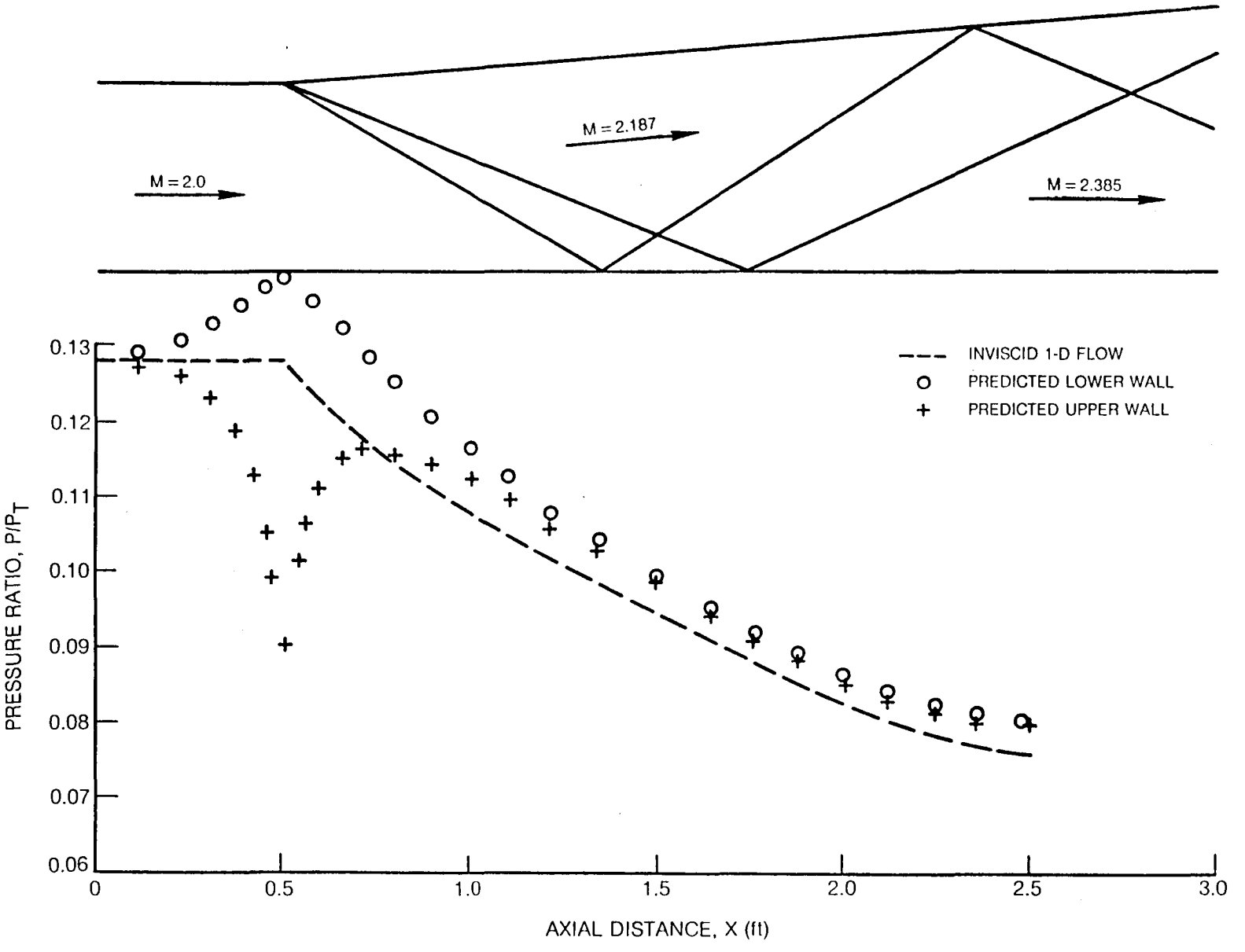

Fig. 4 Comparison of Calculated Wall Pressure with Streamline Curvature Neglected and One-Dimensional Inviscid Flow

84-5-31-2

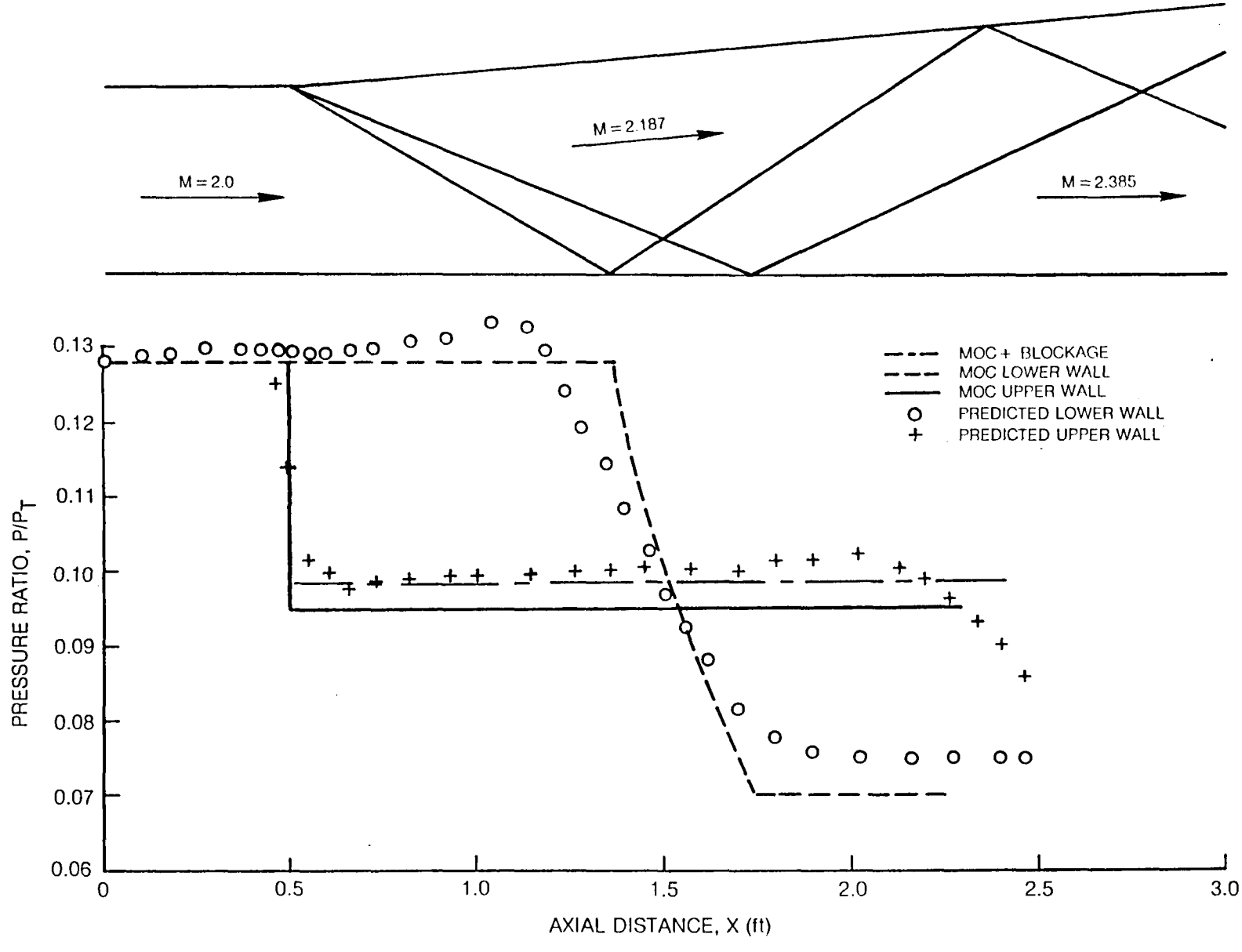

Fig. 5 Comparison of Calculated Wall Pressure with Streamline Curvature Included and the Exact Inviscid Solution from the Method of Characteristics

84-5-31-1

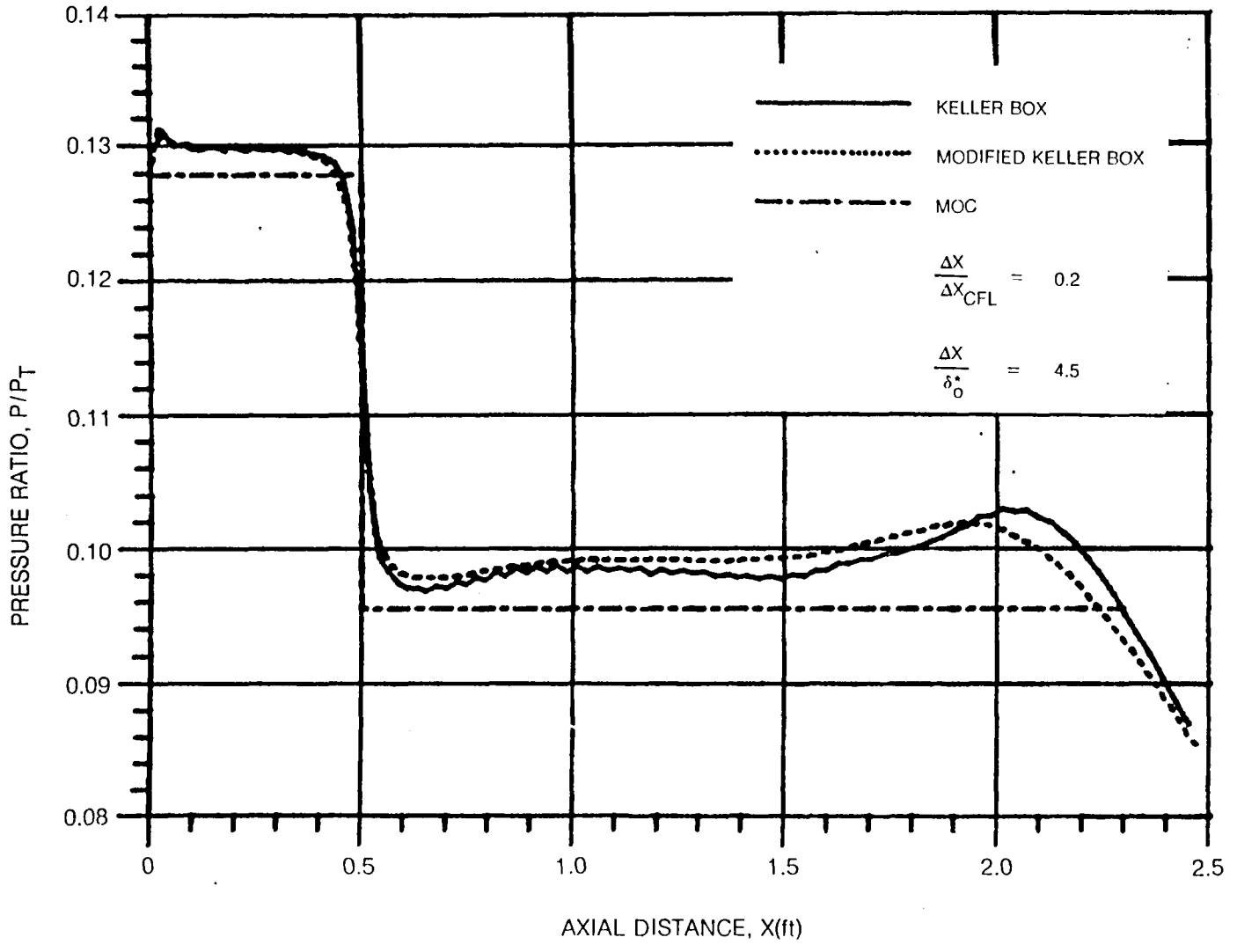

Fig. 6 Comparison of Pressure Distribution for Prandtl-Meyer Expansion Using Keller Box Scheme and Modified Keller Box Scheme

84-7-9-1

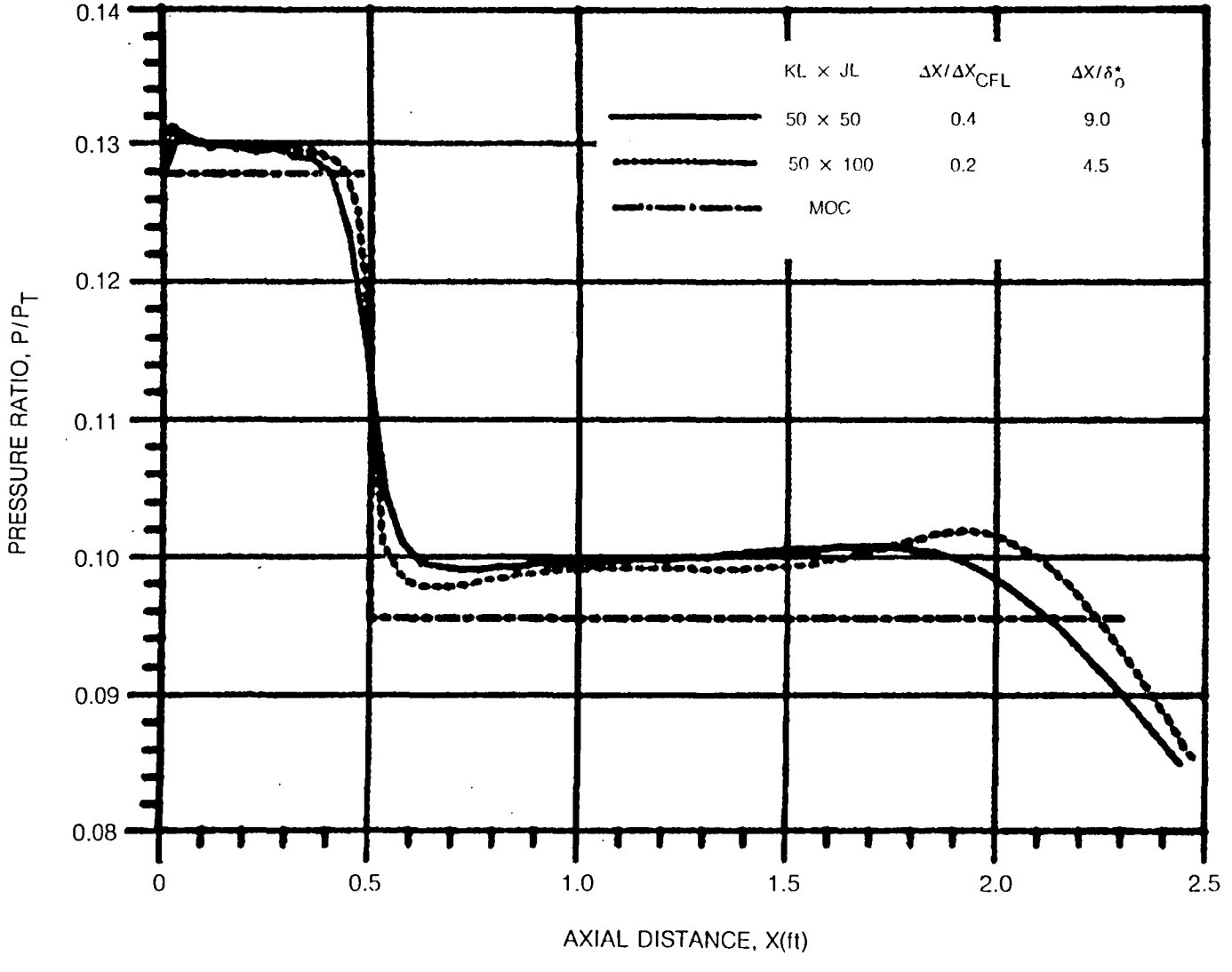

Fig. 7 Effect of Streamwise Step Size on Calculated Wall Pressure Distribution for Prandtl-Meyer Expansion

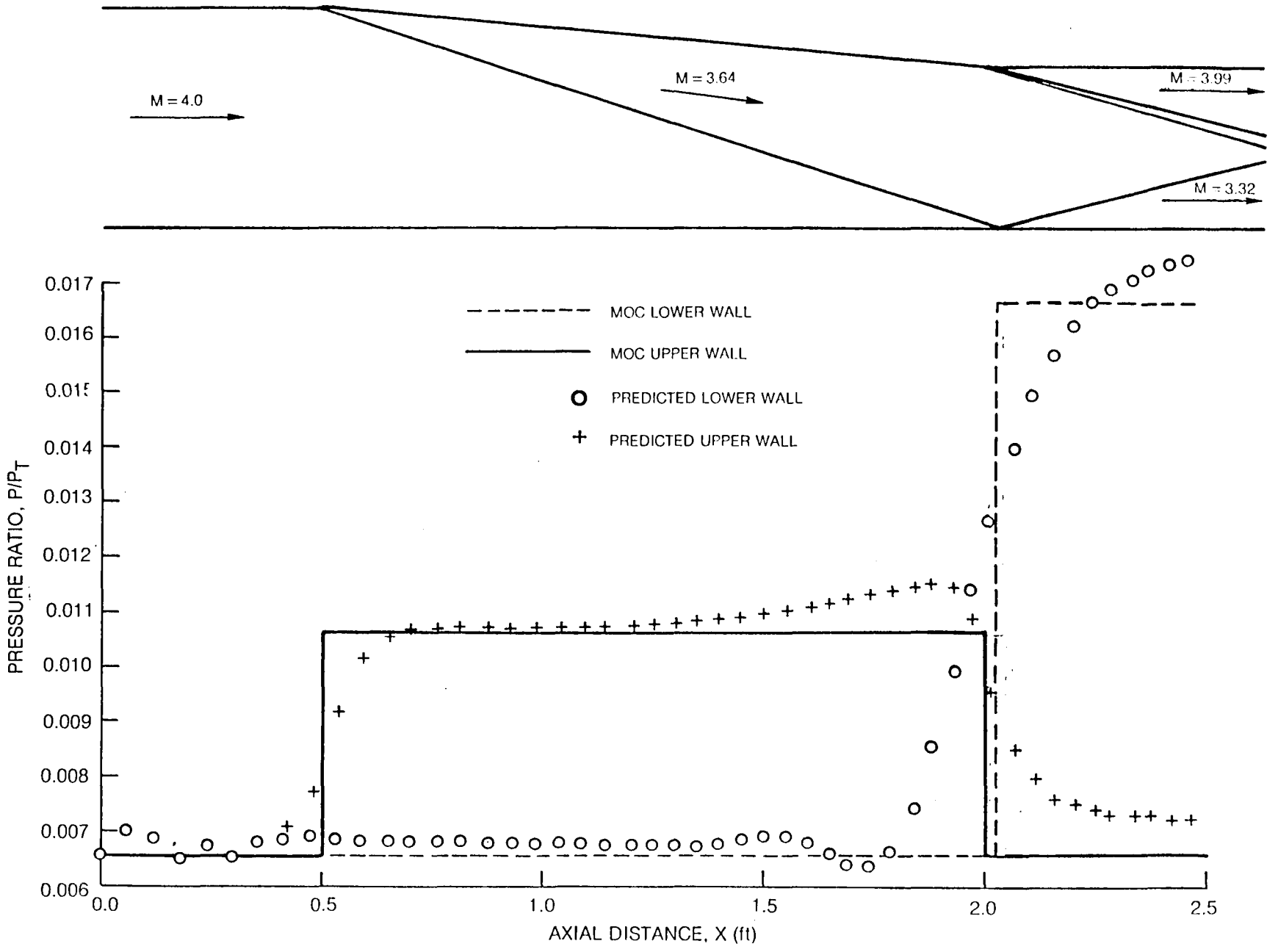

Fig. 8 Comparison of Calculated Wall Pressure with Method of Characteristics

84-6-32-1

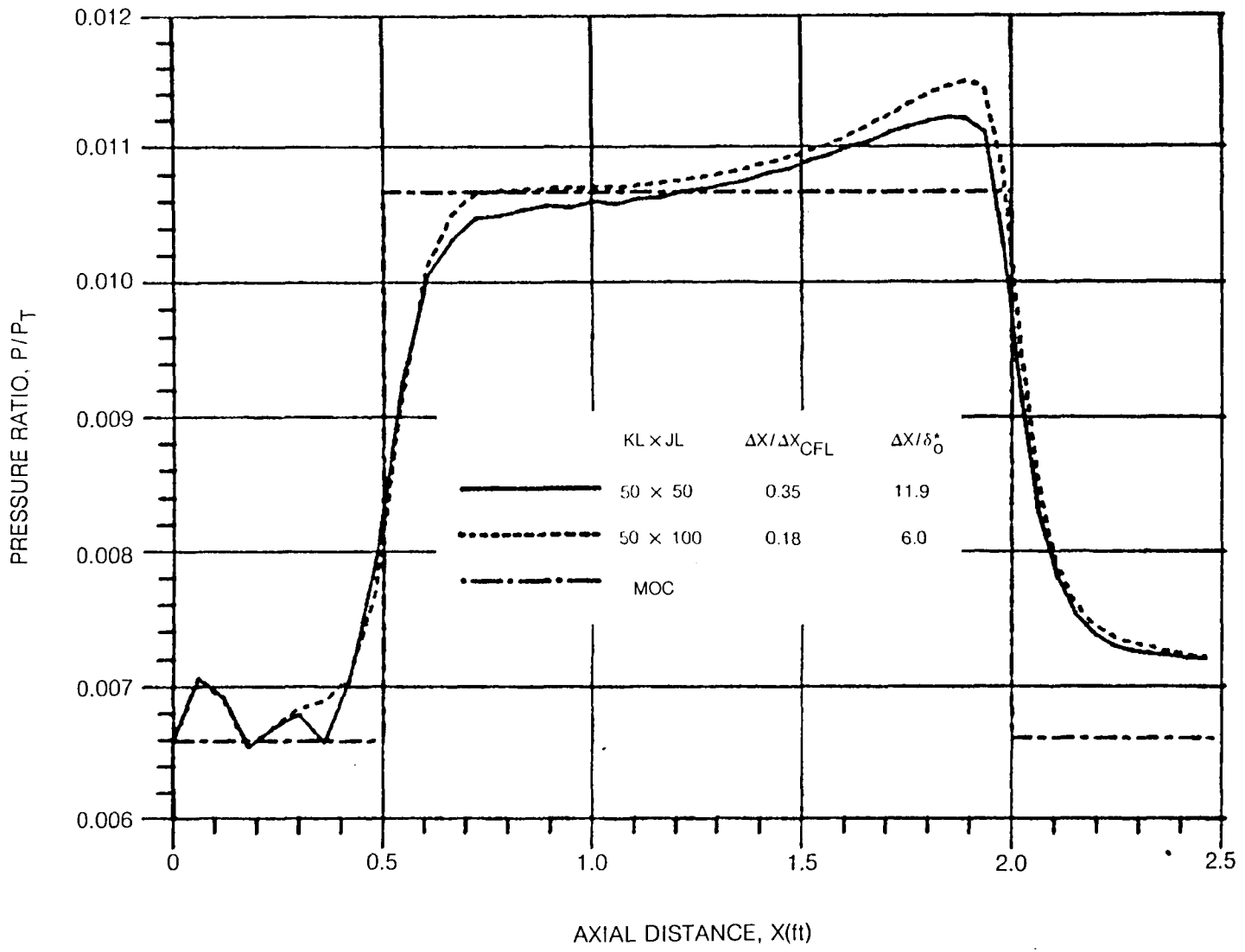

Fig. 9 Effect of Streamwise Step Size on Calculated Wall Pressure Distribution for Shock Wave and Expansion Wave

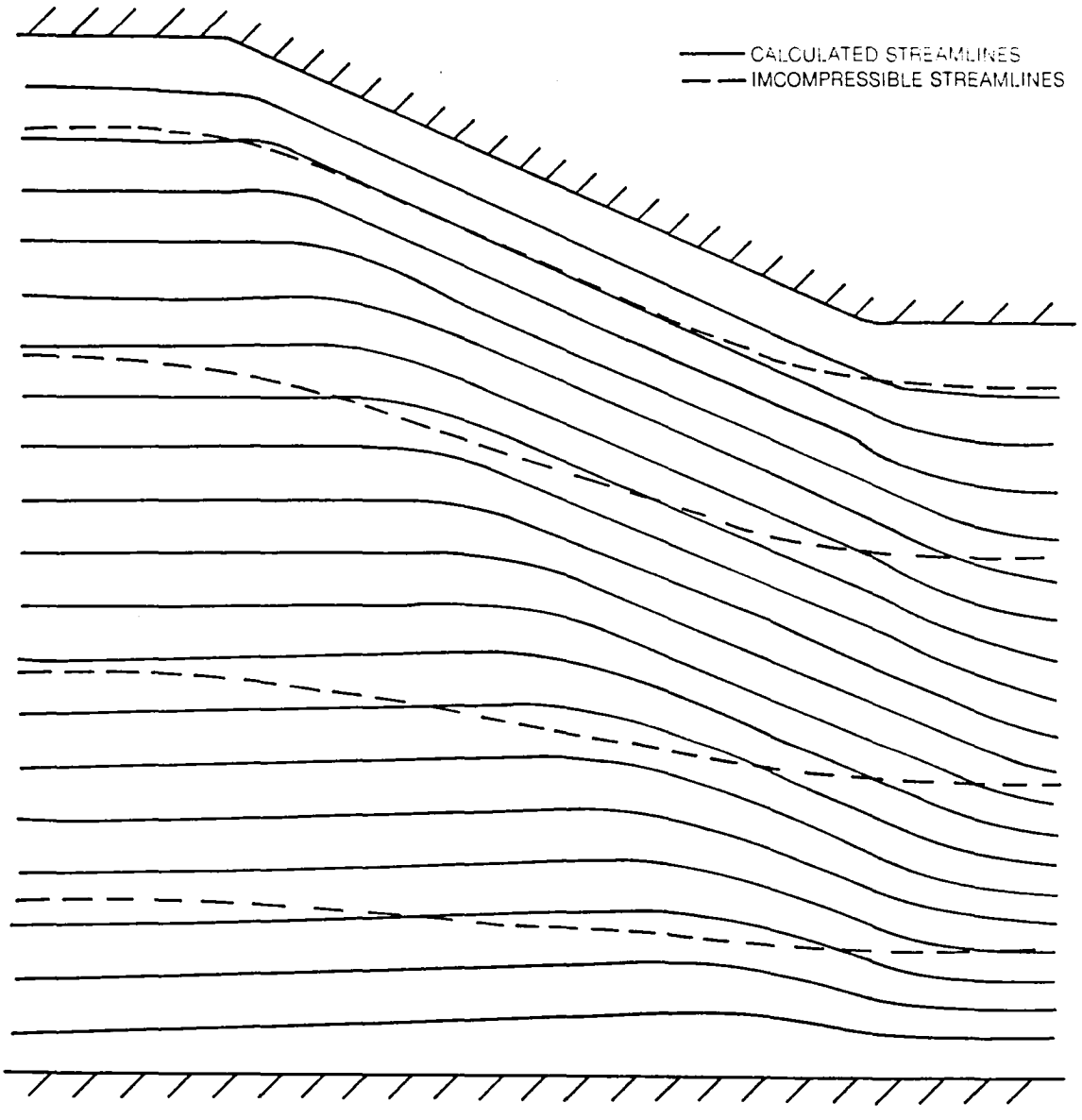

Fig. 10 Calculated Streamlines for Flow with Shock Wave and Prandtl-Meyer Expansion Wave

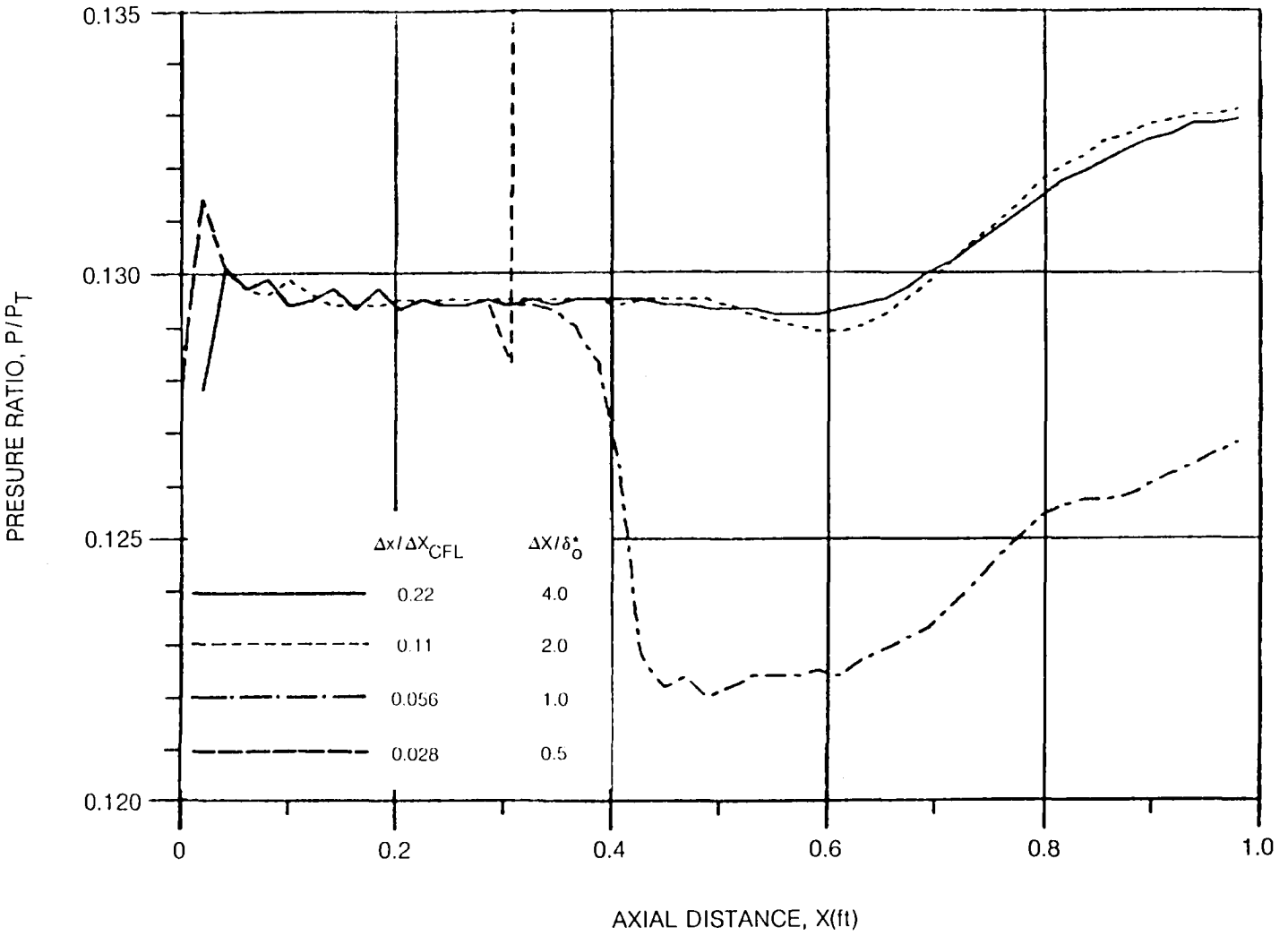

Fig. 11 Effect of Small Step Size on the Calculated Pressure Distribution for Flow in a Straight Duct

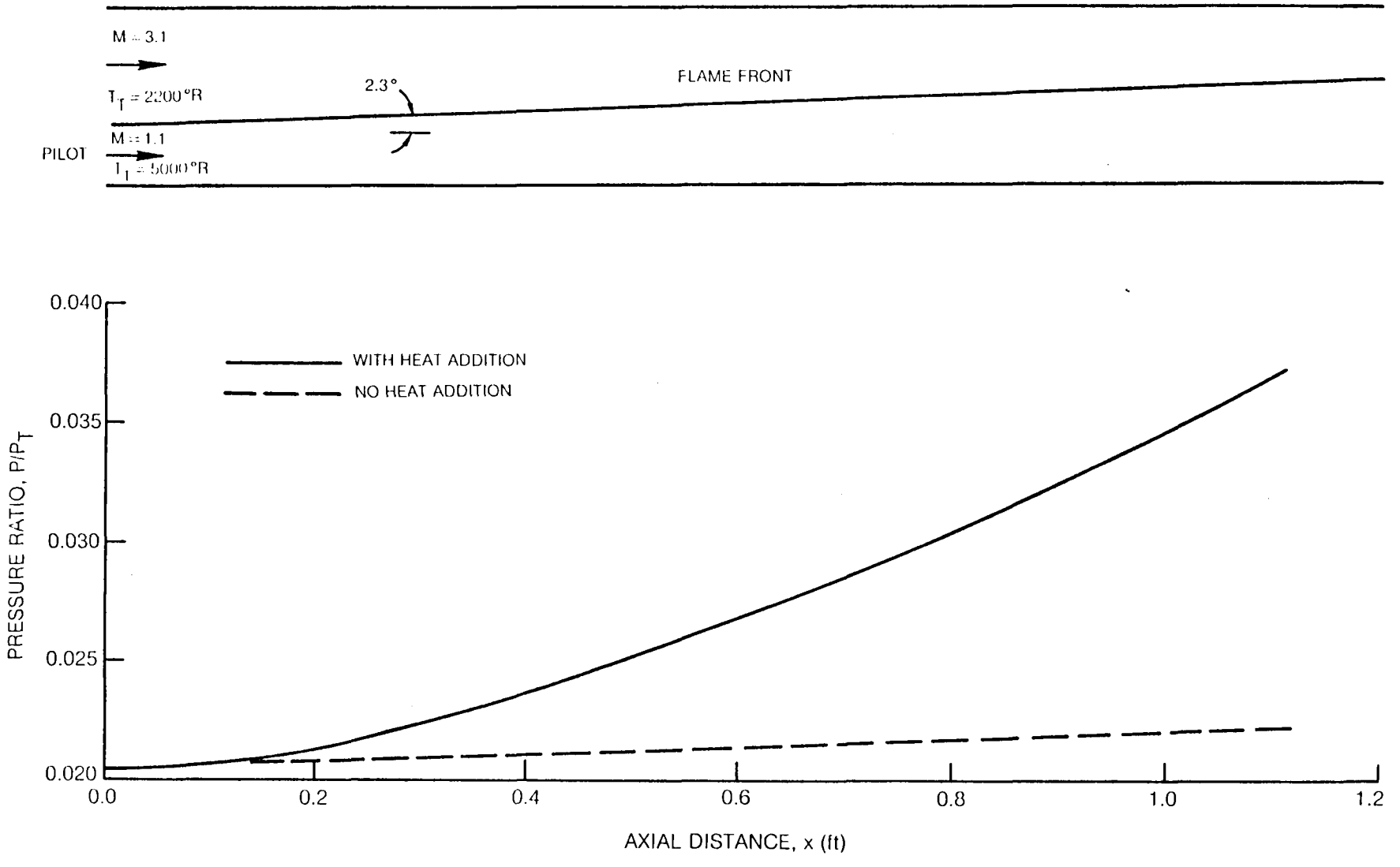

Fig. 12 Comparison of Calculated Wall Pressure With and Without Heat Addition

84-8-51-6

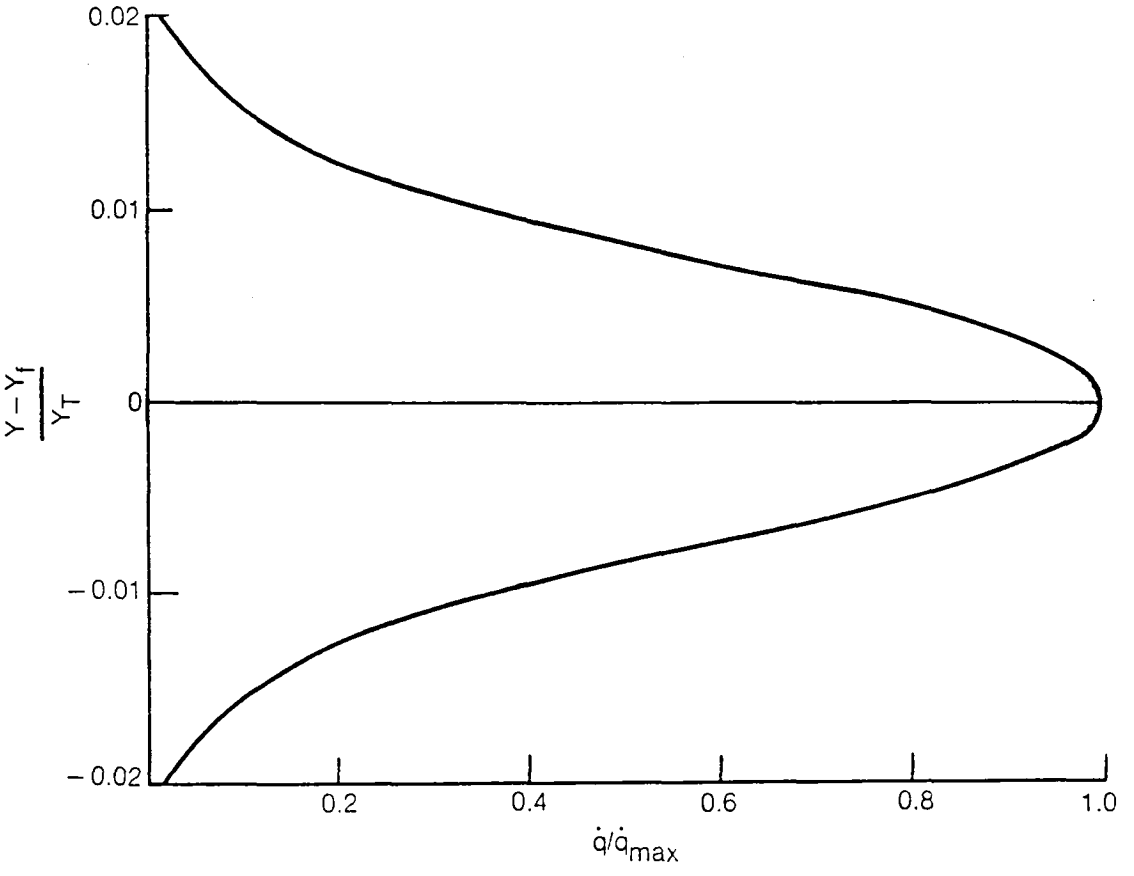

Fig. 13a Normalized Distribution of Heat Input about Flame Midpoint

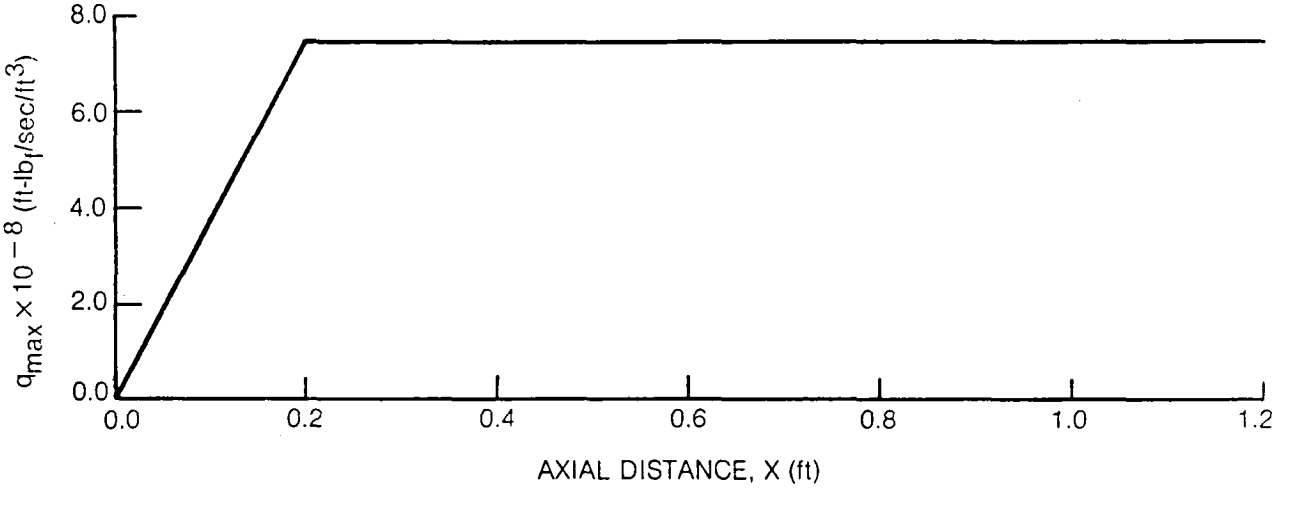

Fig. 13b Maximum Heat Input Along Duct

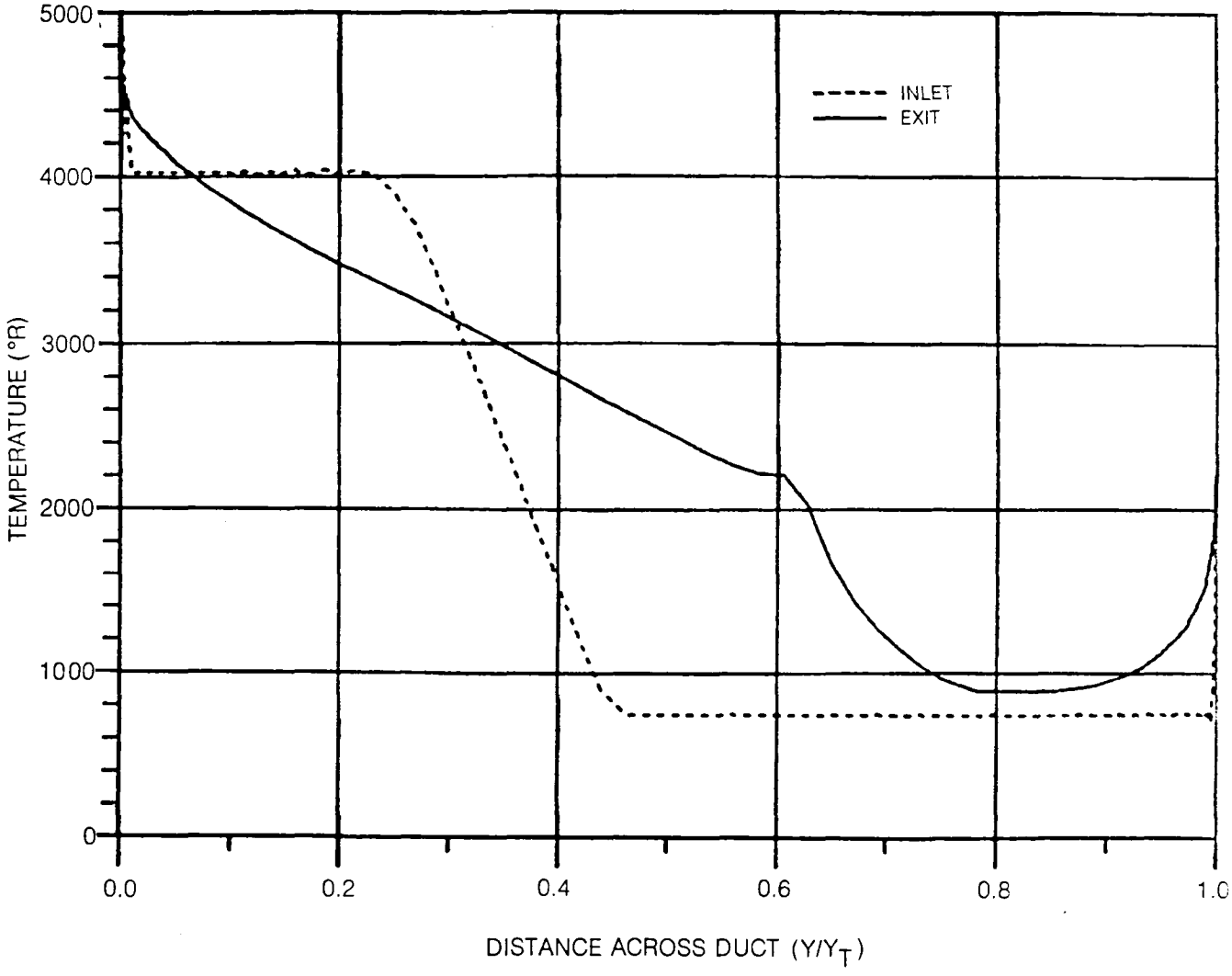

Fig. 14 Inlet/Exit Static Temperature Profiles

84-8-51-4

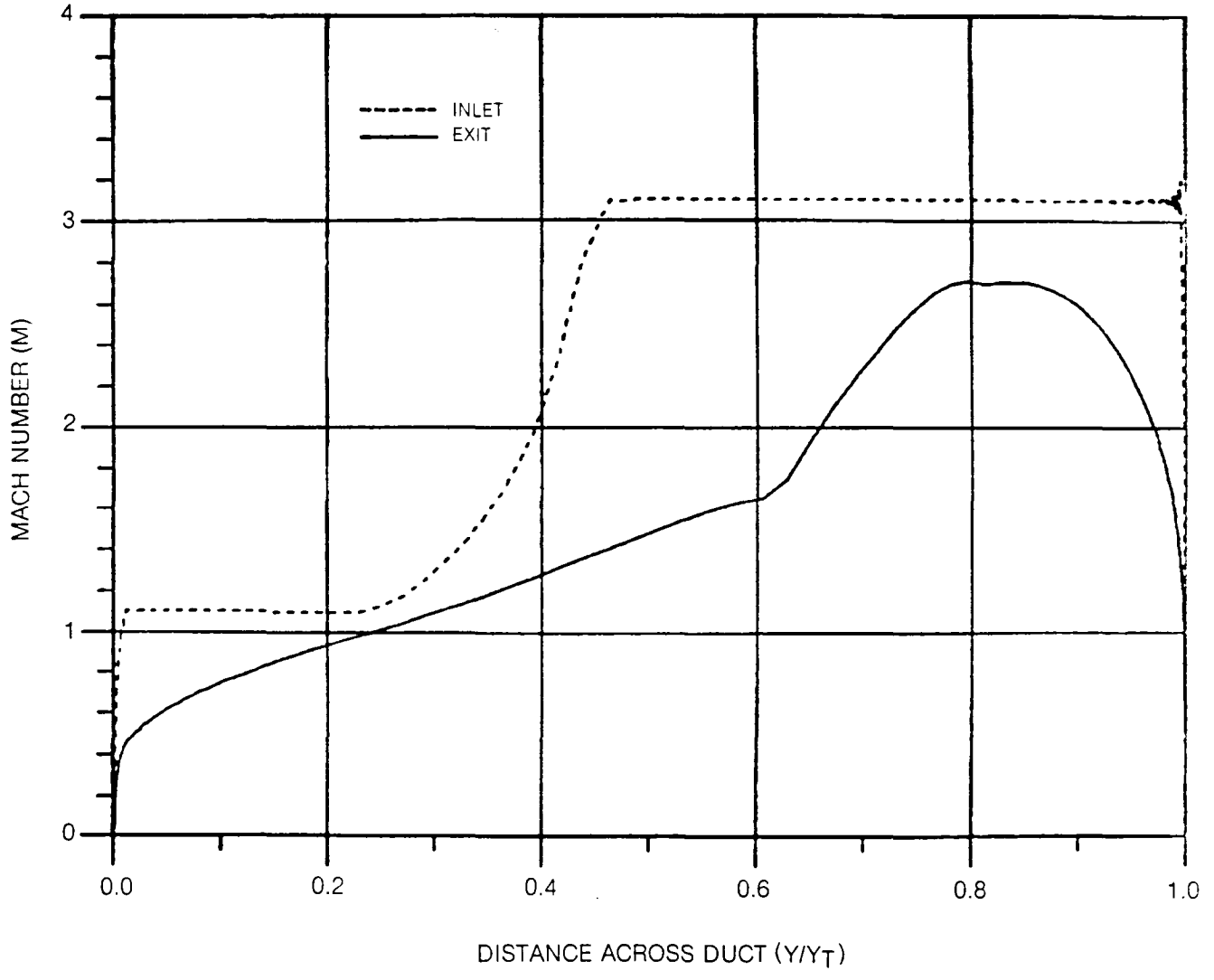

Fig. 15 Inlet/Exit Mach Number Profiles

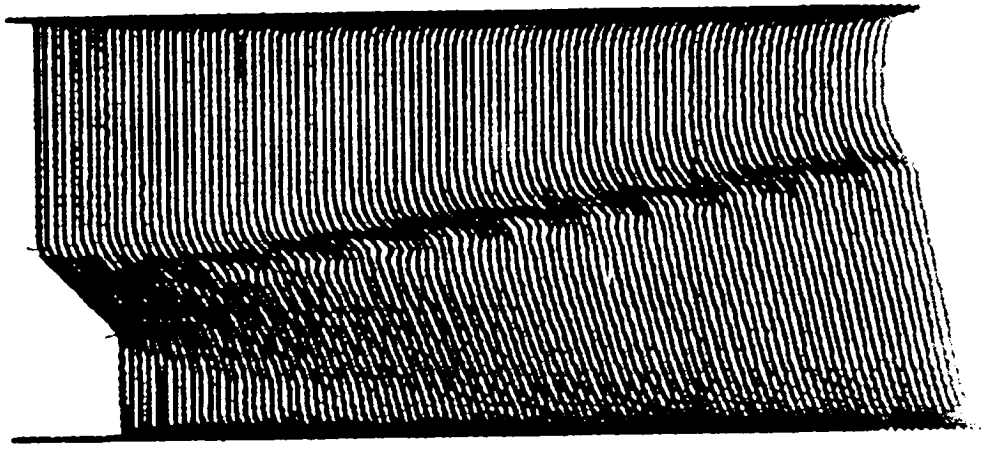

Fig. 16 Static Temperature Profiles Through Duct

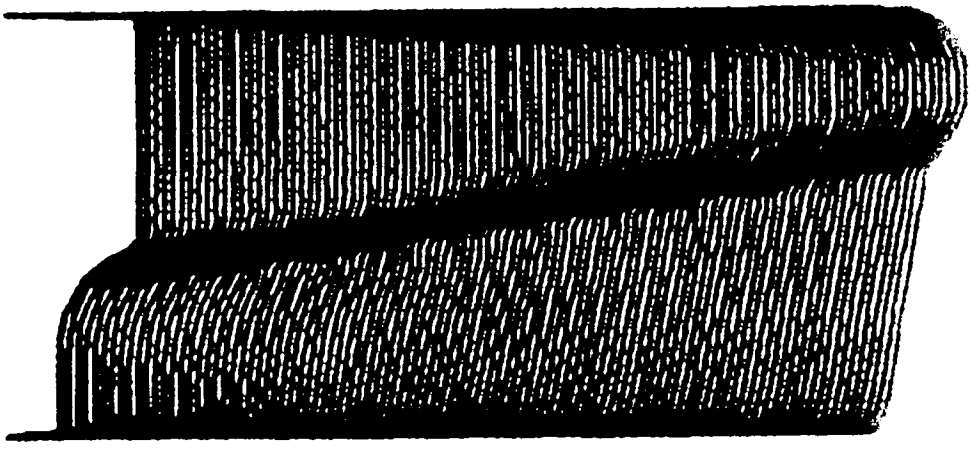

Fig. 17 Mach Number Profiles Through Duct

1. Report No.	2. Government Accession No.	3. Recipient's Catalog No.
NASA CR-172555		

4. Title and Subtitle	5. Report Date
INVESTIGATION OF PARABOLIC COMPUTATIONAL TECHNIQUES FOR INTERNAL HIGH-SPEED VISCOUS FLOWS	April 1985
	6. Performing Organization Code

7. Author(s)	8. Performing Organization Report No.
O. L. Anderson and G. D. Power	R84-956611
	10. Work Unit No.

9. Performing Organization Name and Address	11. Contract or Grant No.
United Technologies Research Center East Hartford, CT 06108	NAS1-17561
	13. Type of Report and Period Covered
12. Sponsoring Agency Name and Address National Aeronautics and Space Administration Langley Research Center Hampton, VA 23665	Contractor report
	14. Sponsoring Agency Code

15. Supplementary Notes

Langley technical monitor: Clayton Rogers
Final Report

16. Abstract A feasibility study has been conducted to assess the applicability of an existing parabolic analysis (ADD-Axisymmetric Diffuser Duct), developed previously for subsonic viscous internal flows, to mixed supersonic/subsonic flows with heat addition simulating a SCRAMJET combustor. A study was conducted with the ADD code modified to include additional convection effects in the normal momentum equation when supersonic expansion and compression waves were present. A set of test problems with weak shock and expansion waves have been analyzed with this modified ADD method and stable and accurate solutions were demonstrated provided the streamwise step size was maintained at levels larger than the boundary layer displacement thickness. Calculations made with further reductions in step size encountered departure solutions consistent with strong interaction theory. Calculations were also performed for a flow field with a flame front in which a specific heat release was imposed to simulate a SCRAMJET combustor. In this case the flame front generated relatively thick shear layers which aggravated the departure solution appearance. Qualitatively correct results were obtained for these cases using the marching technique by suppressing the convective terms in the normal momentum equation. It is concluded from the present study that for the class of problems where strong viscous/inviscid interactions are present a global iteration procedure is required.

17. Key Words (Suggested by Author(s))	18. Distribution Statement
Parabolic Computational Techniques Internal Viscous Flows SCRAMJET Technology	Unclassified - Unlimited

19. Security Classif. (of this report)	20. Security Classif. (of this page)	21. No. of Pages	22. Price
Unclassified	Unclassified	36	

N-305

For sale by the National Technical Information Service, Springfield, Virginia 22161